

*Ab initio* free energy of vacancy formation and mass-action kinetics in vis-active TiO<sub>2</sub>

This article has been downloaded from IOPscience. Please scroll down to see the full text article.

2008 J. Phys.: Condens. Matter 20 022202

(<http://iopscience.iop.org/0953-8984/20/2/022202>)

View [the table of contents for this issue](#), or go to the [journal homepage](#) for more

Download details:

IP Address: 129.252.86.83

The article was downloaded on 29/05/2010 at 07:20

Please note that [terms and conditions apply](#).

## FAST TRACK COMMUNICATION

# *Ab initio* free energy of vacancy formation and mass-action kinetics in vis-active TiO<sub>2</sub>

J Brandon Keith<sup>1,2,3</sup>, Hao Wang<sup>1,2</sup>, Brent Fultz<sup>3</sup> and James P Lewis<sup>1</sup>

<sup>1</sup> Department of Physics, West Virginia University, PO Box 6315, 209 Hodges Hall, Morgantown, WV 26506, USA

<sup>2</sup> Department of Physics and Astronomy, Brigham Young University, N283 ESC Provo, UT 84602, USA

<sup>3</sup> California Institute of Technology, Division of Engineering and Applied Science, Mail Code 138-78, Pasadena, CA 91125, USA

E-mail: [jbrkeith@gmail.com](mailto:jbrkeith@gmail.com)

Received 3 September 2007, in final form 12 November 2007

Published 6 December 2007

Online at [stacks.iop.org/JPhysCM/20/022202](http://stacks.iop.org/JPhysCM/20/022202)

## Abstract

Recent reports have identified bulk defects such as oxygen vacancies as key players in visible-light photoactive TiO<sub>2</sub>. This would imply greater visible light absorption rates may be possible provided effective defect engineering can be achieved. To further this we have developed methods to simulate vacancy formation in bulk TiO<sub>2</sub> using *ab initio* techniques. Initial results of these methods show an entropic reduction in the free energy of vacancy formation of 2.3 eV over a range of 266 K. The use of this result is illustrated by a ‘toy’ mass-action kinetics model which offers insight into vacancy concentration, rate constants, and enthalpy of reaction.

(Some figures in this article are in colour only in the electronic version)

The process of defect formation is of considerable interest. Defects play a significant role in crystalline transport, affect mechanical properties through interactions with dislocations and stacking faults, modify surface chemistry, and alter electrical/optical properties. In transition metal oxides, which play an important role in heterogeneous catalysis, photoelectrolysis, and biocompatibility, defects such as bulk and surface oxygen vacancies often dominate the electronic and chemical surface properties [1].

Prototypical among such oxides is TiO<sub>2</sub> which has oxygen and titanium vacancies, aliovalent Ti interstitials, antisites, and crystallographic shear planes. The nature and quantity of these defects is a subject of long-standing debate with frequently contradictory experimental investigations [2–6]. As an amphoteric semiconductor, TiO<sub>2</sub> has a complex defect phase diagram containing an n–p transition varying with oxygen partial pressure  $p(\text{O}_2)$  and temperature [7].

TiO<sub>2</sub> is also widely used in industry. An important application, photocatalysis, occurs when the strong oxidative

potential of the positive holes oxidizes organics or even oxygen directly. Because of this property it is added to paints, cements, windows, tiles, and many other materials for its sterilizing, deodorizing, and anti-fouling properties, and is even used for hydrolysis or hydrogen production.

One drawback is that UV light is required to activate catalysis due to its wide intrinsic bandgap. Various strategies to improve photo-absorption have been devised to create visible-light activated (vis-active) TiO<sub>2</sub> such as anion doping [8] or chromophore attachment [9, 10] for multielectron injection. Recent precursor [11] and N-dopant [12] studies indicate, however, that manipulation of bulk oxygen vacancy concentration may be one of the most effective ways to increase photocatalytic activity in the visible due to an increase in color centers capable of absorbing at these wavelengths.

To enable rational defect engineering in TiO<sub>2</sub>, a detailed understanding of defect behavior under complex conditions (varying oxygen partial pressure and temperature) is necessary. In this work and a companion publication [14] we introduce

a quantum thermodynamics algorithm to calculate defect parameters and a general statistical mechanics model to gage defect influence on material properties. The quantum methods in particular are difficult to implement because of the large supercells and long-time molecular dynamics runs at various temperatures that are required. However, these are now possible due to the evolution of efficient, linear-scaling electronic structure methods.

The overall statistical mechanics of defect behavior can perhaps be best modeled by the grand canonical ensemble [13] which gives for a TiO<sub>2</sub> crystal containing primarily vacancy defects,

$$j = j_{\text{TiO}_2} + n_{\text{V}}^{\text{O}} F_{\text{V}}^{\text{O}} + n_{\text{V}}^{\text{Ti}} F_{\text{V}}^{\text{Ti}} - T s_{\text{conf}}. \quad (1)$$

$j_{\text{TiO}_2} = f_{\text{TiO}_2} - \mu_{\text{O}} n_{\text{O}} - \mu_{\text{Ti}} n_{\text{Ti}}$  is the grand canonical potential of a perfect TiO<sub>2</sub> crystal per total atoms  $N$ ,  $f_{\text{TiO}_2}$  is the Helmholtz free energy of the perfect crystal per  $N$ ,  $n_{\text{O}}$  ( $n_{\text{Ti}}$ ) is the number of oxygen (titanium) atoms per  $N$ ,  $n_{\text{V}}^{\text{O}}$  ( $n_{\text{V}}^{\text{Ti}}$ ) is the number of oxygen (titanium) vacancies per  $N$ , and  $s_{\text{conf}}$  is the configurational entropy per  $N$ . This ensemble follows the *number* concentration of oxygens which dynamically exchange with an oxygen atmosphere. Thus the oxygen chemical potential  $\mu_{\text{O}}$  is tuned by its partial pressure. The titanium chemical potential  $\mu_{\text{Ti}}$  is fixed by thermodynamic stability relations which near stoichiometry may be approximated as  $\mu_{\text{Ti}} + 2\mu_{\text{O}} = \mu_{\text{TiO}_2}$  but in a more general sense depend on the relative concentration of Ti/O [15].

A key component of this ensemble is the Helmholtz free energy of oxygen vacancy formation  $F_{\text{V}}^{\text{O}}$  which is equivalent to the Gibbs free energy at ambient pressures [16]. This quantity is particularly difficult to determine because of the accurate potentials needed to model vacancies with large electronic restructuring and the difficulty in calculating entropic contributions. Measurements are hampered by the necessity to isolate the effect of removing a single atom. This results in a need for extremely high-quality single crystals and dealing with the effects of material averaging and model limitations when fitting experimental data. In this work we introduce a new approach using powerful *ab initio* thermodynamic methods that efficiently probe bulk oxygen vacancy free energies of formation. This approach should provide greater confidence than force-field based calculations and a more direct means of ascertaining its magnitude than experimental methods such as macroscopic conductivity measurements.

In previous vacancy calculations, the quasi-harmonic approximation to the Helmholtz free energy has frequently been used to calculate  $F_{\text{V}}^{\text{O}}$  [17]. However, this has been shown to be inadequate for much of the temperature span of a solid [18, 19]. Therefore we use nonequilibrium thermodynamic integration [20, 21] (TI), which consists of a molecular dynamics (md) run along a nonphysical path  $\lambda$  between two physical states to find their free energy difference [14, 22]. To apply TI to rutile TiO<sub>2</sub> vacancies, one constructs a composite potential energy surface containing interactions from (1) the perfect crystal, (2) a crystal with one vacancy, and (3) an oxygen atom in a chemical reservoir such as an atmosphere at varying temperature and oxygen partial

pressure. Thus  $V(\lambda) = (1-\lambda)V_{\text{perfect}} \oplus \lambda V_{\text{vacancy}} \oplus \lambda V_{\text{O}_{\text{res}}}$  where  $\lambda \in [0, 1]$ . The vacancy is created by removing the nuclear charge and all electronic terms, although a charged vacancy can also be created.

Nonequilibrium TI is based on equilibrium TI which performs a series of simulations along  $\lambda$  to find the free energy difference,

$$F(\lambda_2) - F(\lambda_1) = \int_0^1 \left\langle \frac{\partial V(\lambda)}{\partial \lambda} \right\rangle_{\lambda'} d\lambda', \quad (2)$$

where  $\langle \rangle_{\lambda'}$  denotes a thermal average at a fixed value of  $\lambda'$ . This difference is the reversible work of vacancy formation. Nonequilibrium TI gives the *irreversible* work,

$$W_{\text{irr}} = \int_0^{t_{\text{sim}}} \left( \frac{d\lambda}{dt} \right)_{t'} \frac{\partial V(\lambda)}{\partial \lambda} \Big|_{\lambda(t')} dt', \quad (3)$$

where  $\lambda$  is a function of simulation time. Here the thermal average occurs continuously while  $\lambda$  is changed adiabatically. One can recover the *reversible* work of vacancy formation as the average between forward and backward TI runs,

$$W_{\text{rev}} = \frac{1}{2} [W_{\text{irr}}(\lambda_1 \rightarrow \lambda_2) - W_{\text{irr}}(\lambda_2 \rightarrow \lambda_1)] = F_{\text{V}}^{\text{O}}. \quad (4)$$

These also serve as upper and lower bounds on  $W_{\text{rev}}$  because of irreversible entropy production<sup>4</sup>.

In regards to our *ab initio* method, we choose FIREBALL, a DFT pseudopotential (LDA/GGA) approach using confined, slightly excited orbitals [23]. Its self-consistent functional allows precalculation of all Hamiltonian integrals and a fast interpolation during runtime which significantly reduces cpu time. The procedure for determining  $W_{\text{rev}}$  has been implemented using a novel client-server algorithm, schematized in figure 1, that creates an electronic structure client for each subsystem. Each subsystem communicates with a server which averages subsystem forces at every time step.

We use a 3d<sup>6</sup>4s<sup>2</sup>4p<sup>0</sup> basis for Ti and a 2s<sup>2</sup>2p<sup>4</sup> basis for O with Troullier Martins pseudopotentials [24] and LDA exchange correlation (XC) [25, 26]. According to recent reports [27, 28], LDA is somewhat preferable to GGA when dealing with vacancies<sup>5</sup>. Previous calculations [29] with this basis reproduced the volume, lattice constants, and atomic positions of rutile and anatase TiO<sub>2</sub> within 0.6% of experimental values [30] and the bulk modulus within 2.4% of experiment [31]. This basis set has also been successfully applied to doping studies of photocatalytic TiO<sub>2</sub> where it gives a 3.05 eV direct rutile bandgap compared to experimental 3.06 eV and a 3.26 eV direct anatase bandgap compared to experimental 3.20 eV (see [32, 33] and references therein). Such accuracy contrasts with the high-cutoff planewave LDA DFT in which the bandgap is underestimated by about 2 eV. The reason for FIREBALL's improved performance is the single

<sup>4</sup> We also attach a harmonic oscillator to the reservoir oxygen ( $V_{\text{O}_{\text{res}}}$  in equation (1)) to prevent singularities in the forces as the oxygen atom wanders through phase space and comes into unphysically close contact with other atoms. Then we subtract the free energy of a harmonic oscillator  $F_{\text{ho}} = -3/(2\beta) \ln[\pi/(\beta m \omega^2)]$  off  $W_{\text{rev}}$  at the end.

<sup>5</sup> We tested GGA (PBE) exchange correlation functionals and did not find as accurate experimental agreement. This validates the conclusions of [27].

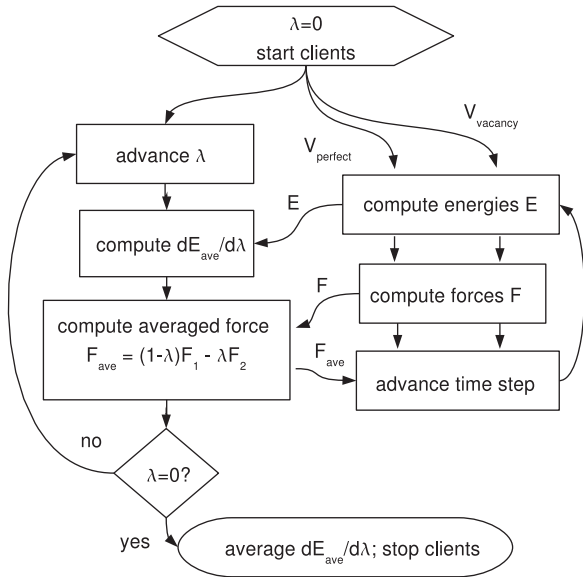


**Figure 1.** Control diagram of electronic structure-based nonequilibrium thermodynamic integration.

numerical local orbital basis which underbinds and the LDA XC which overbinds. Thus this basis is an optimal choice because it is efficient and because errors in certain quantum numerical treatments cancel to make it extremely accurate.

To calculate the vacancy formation free energy in the monovacancy dominating regime we use a 162 atom supercell with a 0.617% atomic vacancy concentration. The energy of vacancy formation is 4.18 eV and is comparable to thermogravimetric experiments of 3.9 eV [34] and 5.6 eV [5, 35]. DFT oxygen surface vacancy calculations give 3.03 eV [36]. Surface vacancies are expected to have slightly lower formation energy so this verifies our calculation. The oxygen chemical potential in equation (1) is assumed to be that of an oxygen atmosphere in its standard state, which can be calculated with the usual thermodynamic expression,

$$\mu_{\text{O}} = \frac{1}{2} \left( E_{\text{O}_2} + kT \left[ \ln \left( \frac{pV_{\text{O}_2}}{kT} \right) - \ln Z_{\text{rot}} - \ln Z_{\text{vib}} \right] \right), \quad (5)$$

where  $V_{\text{O}_2}$ ,  $Z_{\text{rot}}$ , and  $Z_{\text{vib}}$  are given by standard diatomic molecular statistical mechanics [39].

Before calculating  $F_{\text{V}}^{\text{O}}$  as a function of temperature we briefly examine the issue of nonequilibrium simulation length. Performing TI runs for various simulation times allows the convergence analysis shown in figure 2, where each point is the average of 3–6 separate runs and the smoothed data (using moving average filtering) shows the progress to a roughly converged  $F_{\text{V}}^{\text{O}}$ . Examining the plot shows that a nonequilibrium 0.25 ps run is not completely converged but is only 0.1 eV away from a converged 1 ps run. A previous classical nonequilibrium TI study on Ni showed the error between a 1 ps run and a fully converged 8 ps run is 0.05 eV [22]. As 8 ps is prohibitively long for quantum md on such a large system, we add this error to the 0.25 ps run error to estimate the thermodynamic error to be 0.15 eV. Considering the uncertainties within our electronic structure methods we

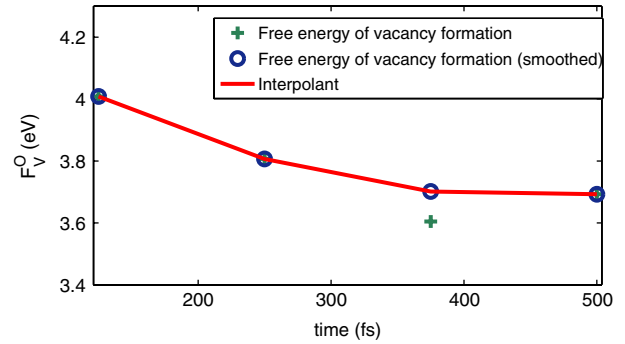


**Figure 2.** Reversible work of vacancy formation  $W_{\text{rev}}$  as a function of nonequilibrium simulation length at 100 K.

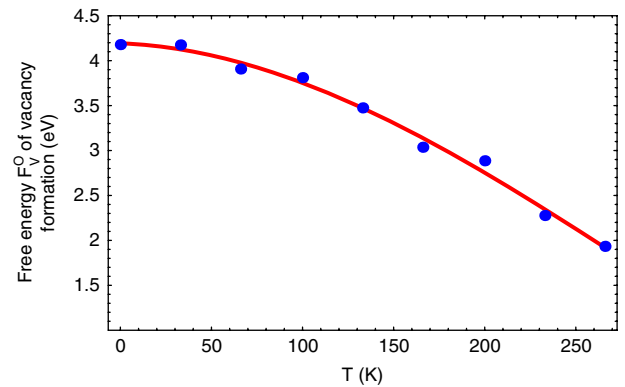


**Figure 3.** *Ab initio* calculation of the oxygen vacancy formation free energy  $F_{\text{V}}^{\text{O}}(T)$  in rutile  $\text{TiO}_2$  as a function of temperature.

consider this acceptable convergence and use it for production runs.

Our initial results for the vacancy formation free energy as a function of temperature are shown in figure 3 using nine data points, each consisting of 5–10 runs. It is expected that such a large number of runs will minimize statistical error. The plot shows a nonlinear decrease in  $F_{\text{V}}^{\text{O}}$  of 2.3 eV (from 4.2 to 1.9 eV) driven by thermal entropic effects. We note the free energy has been referenced to 0 at  $T = 0$  K. Comparison with experimental data at this temperature range is limited, although space charge measurements [37] at higher temperatures give  $G_f \leq 2.1$  eV, which is comparable. We note that the curvature of the free energy shows the departure from the quasi-harmonic approximation. Although these results evidence a considerable drop in the free energy, they include, in addition to vibrational entropy contributions, rather large structural rearrangements throughout the supercell in response to the presence of a vacancy. These displacements in turn lead to additional vibrational entropy contributions from the rest of the atoms. These additional sources of entropy must be considered when comparing with experiment<sup>6</sup>.

<sup>6</sup> We also thank an anonymous reviewer for pointing out a further possibility—it is frequently preferable to generate transition metal pseudopotentials with attention to the ionic environment in which they will be employed (i.e. in a charged state). This has not been done in this work but can be rectified in future work.

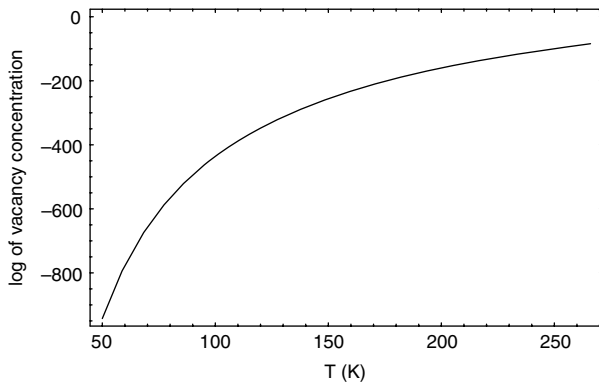


**Figure 4.** Log of vacancy number concentration as a function of temperature.

The quantity of experimental interest is vacancy number concentration  $n_V^0$  which is obtained by minimizing equation (1) with respect to defect number to give

$$n_V^0 = \frac{2}{3} \{ \exp[-(F_V^0 + \mu_O)/kT] \} \{ 1 + \exp[-(F_V^0 + \mu_O)/kT] + \exp[-(F_V^0 + \mu_{Ti} - \mu_O)/kT] \}^{-1} \quad (6)$$

which is valid near standard 1:2 stoichiometry. Equations (1) and (6) form the basis of the point defect gas model because they assume noninteracting vacancies. This model has been validated for many materials over several orders of magnitude in vacancy concentration [16]. Since the denominator does not change significantly with temperature, equation (6) is frequently approximated by  $n_V^0 \propto \exp[-(F_V^0 + \mu_O)/kT]$  and is shown in figure 4 [40, 38].

As previously mentioned,  $F_V^0$  is useful in statistical mechanics models such as in [14]. It may also be employed in a reverse way to a common kinetics model of defects [5–7, 41]. Instead of measuring vacancy concentration to deduce  $F_V^0$  we calculate  $F_V^0$  to assess concentration. Our implementation of this model should be considered qualitative because it (a) assumes oxygen vacancies are the sole defect, when in fact Ti interstitials and crystallographic shear planes also play a major role and (b) uses electron particle kinetics and the ionic picture of  $\text{TiO}_2$ , when in fact electronic states/dynamics are delocalized.

We begin by invoking the law of mass action which gives the formation of vacancies in rutile as  $\text{TiO}_2 \rightleftharpoons \text{TiO}_{2-x} + \frac{x}{2}\text{O}_2^{(g)}$ . In terms of a defect structure primarily involving doubly ionized oxygen vacancies this can be rewritten as  $\text{O}_i^{2-} \rightleftharpoons \text{V}_O^{\cdot\cdot} + \frac{x}{2}\text{O}_2^{(g)} + 2e$ , where  $\text{O}_i^{2-}$  is an oxygen ion in a normal lattice position and  $\text{V}_O^{\cdot\cdot}$  is an oxygen vacancy from which the two electrons normally bound near it in the ionic picture of  $\text{TiO}_2$  have been removed. This concept of ‘removing’ electrons happens implicitly in *ab initio* md during convergence of the wavefunction as charges initially located on titaniums near the vacancy redistribute to other parts of the supercell far away at their free energetic minimum [42]. Forming three rate equations for vacancy formation (rate constant  $k_1$ ), first ionization ( $k_2$ ), and second ionization ( $k_3$ ) and adding them gives the composite relation  $[\text{V}_O^{\cdot\cdot}] = (\frac{1}{4}K)^{1/3} p(\text{O}_2)^{-1/6}$  where  $K = k_1 k_2 k_3$  and  $p(\text{O}_2)$  is the partial pressure of oxygen [5].

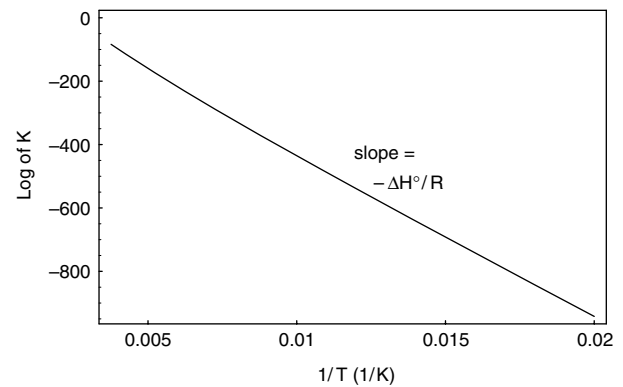


**Figure 5.** Log of the equilibrium constant  $K$  for defect equilibrium in rutile as a function of reciprocal temperature.

From the relation  $F_V^0 \approx \Delta G^0 = -RT \ln(K)$  we can find the rate constant of vacancy formation  $K$ . With this rate constant we can estimate the enthalpy from the van’t Hoff relation  $d \ln K / dT = -\Delta H^0 / RT^2$  by plotting  $\ln(K)$  versus  $1/T$  (figure 5). The slope shows the heat of formation of one mole of vacancies,  $\Delta H^0 = 4.23$  eV, which is comparable to that obtained from previous conductivity measurements (6.3 eV) [41]. Although our formation free energy is quite rigorous, this kinetics treatment is overly simplified so we consider this acceptable experimental agreement. A better approach would be to include titanium interstitials and other types of defects and to use a spatio-temporal treatment such as kinetic Monte Carlo [45].

$\text{TiO}_2$  defects have received much attention from the experimental community. This work represents a small portion of the complementary insight that can be obtained through fast and as-accurate-as-possible local orbital DFT techniques. Such insight could be useful in studying resistivity [3], conductivity, thermoelectric power, diffusion, and redox measurements and further enhance understanding of visible  $\text{TiO}_2$  absorption whether through ultra high vacuum annealing or nitrogen [12], fluorine [43], or cobalt [44] doping. These techniques may also be an effective way to verify that the associated vacancies rather than the dopants themselves are what improve photodegradation [12].

In summary, we have discussed an efficient method for predicting vacancy formation free energies in  $\text{TiO}_2$  from first principles and have explored how this can contribute to various applications in fundamental  $\text{TiO}_2$  defect science and applied surface chemistry.

The calculations were run at the Ira and Mary Lou Fulton Supercomputing Laboratory. This work was supported under the Department of Energy grant DE-FG02-03ER46059 and the National Science Foundation grant DMR-0520547.

## References

- [1] Wendt S, Matthiesen J, Schaub R, Vestergaard E K, Laegsgaard E, Besenbacher F and Hammer B 2006 *Phys. Rev. Lett.* **96** 066107
- [2] Diebold U 2003 *Surf. Sci. Rep.* **48** 53–229

- [3] Li M, Hebenstreit W, Diebold U, Tyryshkin A M, Bowman M K, Dunham G G and Henderson M A 2000 *J. Phys. Chem. B* **104** 4944
- [4] Sasaki J, Peterson N L and Hoshino K 1985 *J. Phys. Chem. Solids* **46** 1267
- [5] Kofstad P 1962 *J. Phys. Chem. Solids* **23** 1579
- [6] Nowotny J, Radecka M and Rekas M 1997 *J. Phys. Chem. Solids* **58** 927
- [7] Nowotny M K, Bak T and Nowotny J 2006 *J. Phys. Chem. B* **110** 16270
- [8] Asahi R, Morikawa T, Ohwaki T, Aoki K and Taga Y 2001 *Science* **293** 269
- [9] Ciofini I 2006 *Theor. Chem. Acc.* **116** 219
- [10] He T and Yao J 2006 *Prog. Mater. Sci.* **51** 810
- [11] Martyanov I N, Uma S, Rodrigues S and Klabunde K J 2004 *Chem. Commun.* **21** 2476
- [12] Batzill M, Morales E H and Diebold U 2006 *Phys. Rev. Lett.* **96** 026103
- [13] Meyer M and Fahnle M 1995 *Phys. Status Solidi* **191** 283
- [14] Keith J B, Lucas M, Fultz B F and Lewis J P 2007 Generalized statistical mechanics of point defects, in preparation
- [15] Hu Q M, Yang R, Hao Y L, Xu D S and Li D 2004 *Phys. Rev. Lett.* **92** 185505–9
- [16] Kraftmakher Y 1998 *Phys. Rep.* **299** 79–188
- [17] Clark S J and Ackland G J 1993 *Phys. Rev. B* **48** 10899
- [18] Sandberg N and Grimvall G 2001 *Phys. Rev. B* **63** 184109
- [19] Foiles S M 1994 *Phys. Rev. B* **49** 14930
- [20] Chipot C and Pearlman D A 2002 *Mol. Simul.* **28** 1
- [21] Pearlman D A 1994 *J. Phys. Chem.* **98** 1487
- [22] de Koning M, Ramos de Debiaggi S and Monti A M 2004 *Phys. Rev. B* **70** 054105
- [23] Lewis J P, Glaesemann K R, Voth G A, Fritsch J, Demkov A A, Ortega J and Sankey O F 2001 *Phys. Rev. B* **64** 195103
- [24] Troullier N and Martins J L 1991 *Phys. Rev. B* **43** 1993–2006
- [25] Ceperley D M and Alder B J 1980 *Phys. Rev. Lett.* **45** 566
- [26] Perdew J P and Zunger A 1981 *Phys. Rev. B* **23** 5048
- [27] Carling K, Wahnstrom G, Mattsson T R, Mattsson A E, Sandberg N and Grimvall G 2000 *Phys. Rev. Lett.* **85** 3862
- [28] Kurth S, Perdew J P and Blaha P 1999 *Int. J. Quantum Chem.* **75** 889
- [29] Jelinek P, Wang H, Lewis J P, Sankey O F and Ortega J 2005 *Phys. Rev. B* **71** 235101
- [30] Burdett J K, Hughbanks T, Miller G J, Richardson J W and Smith J V 1987 *J. Am. Chem. Soc.* **109** 3639
- [31] Arlt T, Bermejo M, Blanco M A, Gerward L, Jiang J Z, Olsen J S and Recio J M 2000 *Phys. Rev. B* **61** 14414
- [32] Wang H and Lewis J P 2005 *J. Phys.: Condens. Matter* **17** L209
- [33] Wang H and Lewis J P 2006 *J. Phys.: Condens. Matter* **18** 421
- [34] Forland K S 1959 *Tionde Nordiske Kemistmotet* (Stockholm: Almqvist)
- [35] Forland K S 1964 *Acta Chem. Scand.* **18** 1267
- [36] Rasmussen M D, Molina L M and Hammer B 2004 *J. Chem. Phys.* **120** 988
- [37] Ikeda J A S, Chiang Y M, Garatt-Reed A J and Van der Sande J B 1993 *J. Am. Ceram. Soc.* **76** 2447
- [38] Smargiassi E and Madden P A 1995 *Phys. Rev. B* **51** 117
- [39] Van de Walle C G and Neugebauer J 2004 *J. Appl. Phys.* **95** 3851
- [40] McCarty K F, Nobel J A and Bartlet N C 2001 *Nature* **412** 622
- [41] Son J and Yu I 1996 *Korean J. Ceram.* **2** 131
- [42] Capron N and Boureau G 2003 *Int. J. Quantum Chem.* **99** 677
- [43] Li D, Haneda H, Labhsetwar N K, Hishita S and Ohashi N 2005 *Chem. Phys. Lett.* **401** 579
- [44] Jaffe J E, Droubay T C and Chambers S A 2005 *J. Appl. Phys.* **97** 073908
- [45] Fu C C, Torre J D, Williams F, Bocquet J L and Barbu A 2005 *Nat. Mater.* **4** 68